Performance comparison of three storage systems for mild HEVs using PHIL simulation

R. Trigui, B. Jeanneret, B. Malaquin, C. Plasse

IEEE Transactions on Vehicular Technology, Vol 58 Issue 8,Oct. 2009, pp 3959 - 3969
DOI: 10.1109/TVT.2009.2028146

http://ieeexplore.ieee.org/xpl/RecentIssue.jsp?punumber=25

Performance Comparison of Three Storage Systems for Mild-HEVs using PHIL Simulation

Rochdi Trigui, *Member*, *IEEE*, Bruno Jeanneret, Bertrand Malaquin and Cedric Plasse

***Abstract*-HEVs would contribute to the energy saving and GHE reduction if they are launched massively on the market. A notable effort has been done in simulation in order to optimize the energy consumption and the component sizing. PHIL simulation could be a further step in order to obtain more realistic performance and to compare different solutions including economic aspects. This paper deals with the implementation on a high dynamic test bench of a diesel Mild-hybrid parallel HEV using PHIL technique. Three configurations, corresponding to different energy storage systems, have been tested in the same conditions. Power, energy, consumption and pollutant emission performance, measured on the test bench, are compared and discussed.**

***Index terms* - Hybrid Electric Vehicle, Hardware In the Loop, fuel consumption, diesel engine.**

I. INTRODUCTION

Hybrid Electric Vehicles (HEVs) represent an interesting alternative to the conventional vehicles in terms of fuel economy and lower atmospheric pollutants emission. For the midterm, charge-sustaining based HEVs allow the use of relatively small batteries and/or super-capacitors, the main energy gain comes from the energy recovery during deceleration phases. For the long term, plug-in HEVs using charge depleting strategies would introduce electric energy as a share of consumption to reduce CO2 emission and petroleum dependency. However, price and reliability of the storage systems for this type of vehicle remains the most critical problem for a large market introduction. Consequently, each hybrid solution should be optimized in term of cost versus energetic performance.

R. Trigui, B. Jeanneret and B. Malaquin are with the Transport and Environment Laboratory of the French National Institute on Transport and Safety Research (INRETS). 25 avenue F. Mitterrand. 69675 Bron, France. (e-mail rochdi.trigui@inrets.fr). R. Trigui is also with the French network MEGEVH dealing with HEVs modelling and control.
C. Plasse is with Valeo Electric Systems. 2, rue Boulle, Créteil, France. (e-mail cedric.plasse@valeo.com)

As several hybrid topologies exist and can operate in charge sustaining mode as well as in charge depleting, an important number of solutions, mainly if we consider the hybridization rate as a variable [1, 2, 3], should be investigated and optimized. For this purpose, simulation has been identified as a good approach and many software based on system modelling have been developed for HEVs simulation and gave different fuel economy results according to the type and size components of the vehicle [4, 6, 7, 27, 28].
Nevertheless, realistic performance of critical components is difficult to obtain only by simulation (Pollutant Emission, storage system behaviour, cold start effect…). This can affect the accuracy of the simulation results mainly when the optimization methods used in the energy management depend strongly on the models parameters, which is usually the case [21, 22].
PHIL (Power Hardware In the Loop) simulation constitutes an interesting intermediate step, before prototype building, in order to obtain more realistic performances than pure simulation [8]. In this concept, one or more components of the powertrain can be tested on a bench while the other components are simulated. The actual component receives request from the Real Time simulation process and communicates information from sensors installed.
Different applications: EVs and their components [8, 9, 10], wind energy [11, 12], HEVs and their components [13, 14, 15, 16] have used successfully the PHIL technique mainly for control development. Our approach here is to use a PHIL which combines dynamic and control tests with a necessary consumption and pollutant emission measurements in order to compare more precisely different powertrains and different energy management strategies. For example, diesel hybrid would be a very interesting solution for CO2 reduction if the NOx emissions are drastically reduced according to the European future standards. This approach is cost effective and allows fair assessment by mastering test conditions while testing a large panel of the possible vehicle use (standard, urban, road, highway).
This paper highlights how we can apply the PHIL principle in order to test the ICE, the Electric machine and the storage systems in a parallel mild-hybrid configuration. One of the main advantages of this approach demonstrated here is a more effective assessment than pure simulation of different solutions by exchanging components for a same configuration and same conditions. For the special case of the electric storage systems, the near actual test allowed by the PHIL simulation presented here is very useful for analysing their behaviour during different entire driving cycles collected from actual vehicle uses [17].

Three storage systems, two batteries and an ultracapacitor, are tested in the PHIL mild hybrid configuration and the performance are compared in term of power, energy and fuel economy of each hybrid solution. The first section presents the three HEVs configurations and the reference vehicle used for comparison. Then the PHIL principle is detailed and its implementation described. And finally the experimental results are given and discussed.

II. REFERENCE VEHICLE AND HEVS FEATURES

In order to appreciate the fuel economy allowed by each of the three HEVs corresponding to the three storage systems, we will consider a conventional vehicle as a reference. This vehicle is a passenger car, Compressed Ignition Direct Injection (CIDI) powered, with a conventional transmission consisting of a two-plate friction clutch, a five manual gear box and a final ratio. The Mild-hybrid HEVs are two clutched parallel hybrid which have the same body and the same ICE than the reference vehicle (figure 1). The tables I and II summarize the characteristics of the reference vehicle and the added elements for each of the HEVs (called from now: HEV1, HEV2 and HEV3).

TABLE I
COMMON ELEMENTS FEATURES

	value	unit
Chassis		
Mass	780	kg
Sf	1.89	m2
Cx	0.35	/
Roll. Coef.	0.0106	/
Wheels		
Number	4	/
Inertia	0.7	Kgm2
radius	0.28	m
ICE		
type	Diesel CIDI	
displacement	1500	cm3
Max. Power	60 @4000	kW@rpm
Max. Rot. speed	5000	rpm
Gear box		
	ratio	efficiency
1st gear	3.72	0.90
2nd gear	2.05	0.97
3rd gear	1.32	0.98
4th gear	0.97	0.98
5th gear	0.75	0.98
Final ratio	3.29	0.97
Clutch		
Radius	0.1	m
Friction coeff.	0.28	/

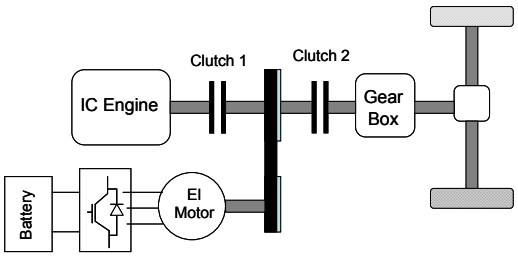

Fig. 1: Hybrid Power train considered

For HEV1, the electric motor is a modified conventional claw-pole alternator. The modifications consist of:

- rewinding the stator coil in order to have more important transient power;
- Active temperature control of the stator winding.

For HEV2 and HEV3, the electric motor is a synchronous motor with a hybrid excitation. The rotor is composed by both coils and permanent magnets. This allows a large area of torque/speed functioning associated to a quite good efficiency.

Table II
HEVs SPECIFIC ELEMENTS FEATURES

		HEV1	HEV2	HEV3
DC/AC inverter	type	MOSFET	MOSFET	MOSFET
	Manufacturer	Valeo	Valeo	Valeo
	DC Voltage	24-50 V	24-50 V	24-50 V
Electric Motor	type	Wound SM	PMSM +wound	PMSM +wound
	Manufacturer	Valeo	Valeo	Valeo
	Peak Power	9 kw	15 kW	15 kW
Storage System	type	V. R. L. A. battery	Ni-MH battery	DLUltra-capacitor
	Manufacturer	Exide	Saft	Maxwell
	Peak Power	10 kW	15 kW	> 18 kW
	Voltage	36 V (3*12V)	36V (3*12V)	48V
	Capacity	30 Ah	34 Ah	144 F
	cooling	air	water	air
	Estimated* number of cycle @20% SOC	300-1000	500-2000	500k- 1M

* Data source [18]

III. PHIL SIMULATION

A. *Parallel HEV PHIL implementation :*

As the conventional reference vehicle PHIL model is a part of the whole HEV model, we only describe here the implementation of the parallel HEV.

The experimental test bench is based on an industrial high dynamic load from AVL[1] with a maximum power of 120 kW. This load consists of an Induction motor generator (*dyno*) fed by bidirectional AC/DC DC/AC inverters and develops a Torque of ±250 Nm with a high dynamic response (torque response time < 3 ms [19]) (Fig 2). For the considered configuration, the simulated parts are developed under VEHLIB [4, 5] (Fig. 3.) and corresponding models are briefly described in the next sections.

The actual components under test are:

- the diesel ICE
- the electric storage system
- The electric machine (EM) and its inverter
- The clutch 1.

[1] Austrian test bench manufacturer.

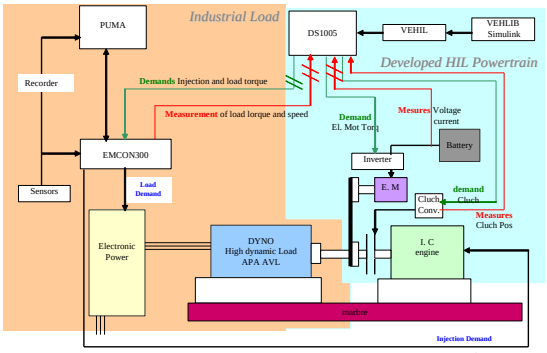

Fig. 2. Test bench synoptic in the parallel hybrid configuration.

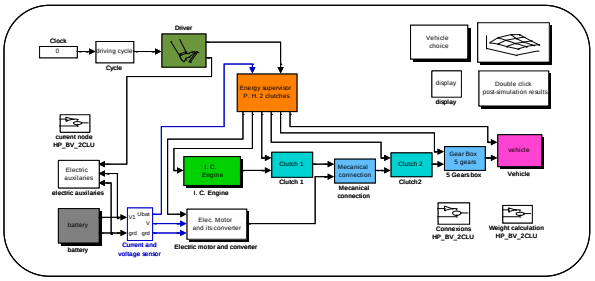

Fig. 3. All simulation VEHLIB-based model of the parallel Hybrid vehicle.

Simulink® models of the simulated components are implemented in a real time version of VEHLIB [20] which assures the interface with the measured signals as inputs and control signals as outputs (Fig.2). The PHIL model is then compiled and executed using a RTW and DS1005&DS2201 Dspace® configuration.

B. Chassis model

We consider here only the longitudinal motion of the vehicle, so the dynamic equation is reduced to:

$$J_{veh}\frac{d\omega_r}{dt} = T_r - T_f - T_b \qquad (1)$$

Where T_r is the wheel torque developed by the motor and the ICE, T_f is the load torque calculated from the resistant forces (rolling, aerodynamic and slope), T_b is the mechanical brakes torques and ω_r is the wheels rotation speed.

J_{veh} is the overall vehicle inertia brought back to the wheels. When the two clutches are locked, this parameter is given by :

$$J_{veh} = M_{veh}R_{wheel}^{\ 2} + 4J_{wheel} + \eta_{gear}(k)\rho_{gear}(k)^2 J_{ice} + \eta_{gear}(k)\eta_{belt}(\rho_{gear}(k)\rho_{belt})^2 J_{em} \qquad (2)$$

where M_{veh} is the vehicle mass, R_{wheel} is the wheel radius, J_{wheel} is one wheel inertia, $\eta_{gear}(k)$ and $\rho_{gear}(k)$ are respectively the efficiency and the gear ratio of the gear number k, η_{belt} and ρ_{belt} are respectively the efficiency and the ratio of the belt, J_{ice} is the ICE inertia and J_{em} is the EM inertia.

C. Gear Box Model

The gear box model is a mechanical transformer with variable ratio ρ_{gear} depending on the gear number k. Torques and speeds are calculated according to equations :

$$\begin{cases}\omega_{gear} = \rho_{gear}(k)\omega_r \\ T_r = \rho_{gear}(k)T_{gear}\eta_{gear}(k)\end{cases} \quad k = 1,2...5 \qquad (3)$$

D. Clutch model and its validation

Two states of the clutch are considered: locked and slipping mode. For the locked mode, torques, inertia and speeds are transmitted without loss. For the slipping mode, the torques on the primary (T1) and the secondary (T2) of the clutch are given by:

$$T_1 = T_2 = 2\,F_n\,R_{clutch}\,\mu\,sign\left(\Omega_1 - \Omega_2\right) \qquad (4)$$

where R_{clutch} is the radius of the clutch plate, Ω_1 and Ω_2 are the primary and the secondary rotating speeds of the clutch, μ is the friction coefficient and an approximated expression of the normal force, function of the clutch pedal position P_{clutch} is given by :

$$F_n = F_{n\_max}\left[1 - \sqrt{1 - \left(\frac{p_{clutch}}{100} - 1\right)^2}\right] \qquad (5)$$

More details of the clutch model are given in [23].

As the clutch is a sensitive component with important transient torques during gear shifting phases, a special care has been given to its model validation and control [24]. Figures 4 and 5 show a comparison between simulation and experimental results.

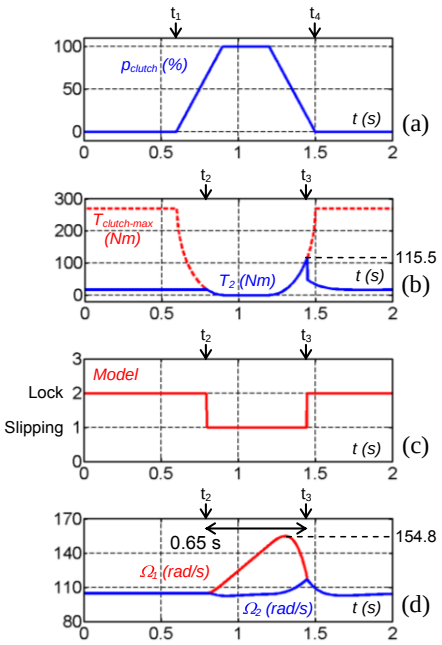

Fig. 4. Simulation results of the transmission with clutch: position of the clutch release bearing (a), clutch torque and maximal clutch torque (b), model used (c), rotation speeds (d)

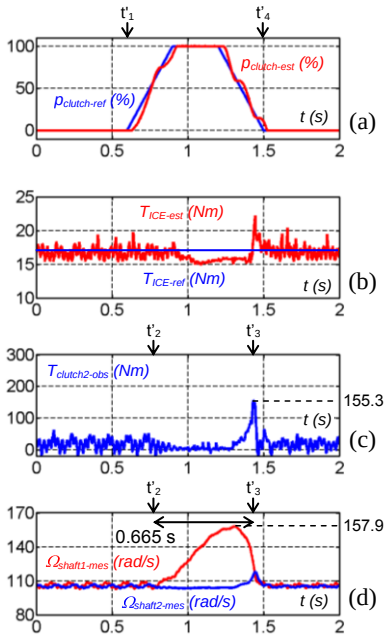

Fig. 5. Experimental results of the transmission with clutch: position of the clutch release bearing reference and estimated (a), ICE torque estimated (b), clutch torque observed (c), rotation speeds measured (d)

Where T_{ICE} is the ICE torque connected to the secondary of the clutch, and $T_{clutch-\max}$ is the maximum transmissible torque given by the expression (4).

Except the maximum torque value underestimated in simulation (fig. 5 (c)), we can note a good agreement between simulation and experiments.

E. Driver model

The driver model is a simple PI controller applied to the vehicle speed, the reference torque is given by:

$$T^*_{driver} = P(\omega^*_r - \omega_r) + I\int(\omega^*_r - \omega_r)dt \qquad (6)$$

Where P is the proportional coefficient and I is the integral coefficient.

F. Energy Management

In this first step of implementation, Energy management, verified by simulation in the model shown in Fig. 3, consists of a rule based algorithm. More advanced methods have been studied by simulation [26] and their implementation will be the subject of a next paper.

In the work presented here, the following functions have been implemented:

- stop/start operation of the ICE.
- maximum Energy recovery during deceleration
- electric mode when the power demand is lower than a given threshold
- boost capabilities while extreme accelerations
- serial flux (battery recharging through the ICE).

As it has been demonstrated in previous studies using dynamic programming [21], this last function does not give notable energy gain in our case. It is used here to maintain battery SOC in a given interval. Therefore, the corresponding simplified algorithm is described on the figure 6.

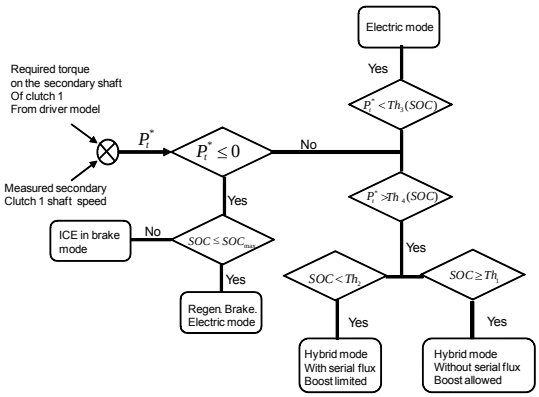

Fig. 6. Simplified Energy management algorithm diagram

Where P_t^* is the traction power demand, Th_1 and Th_2, thresholds for battery and Ultra-capacitors *SOC*, and Th_3 and Th_4 the power demand thresholds for the ICE starting/stopping.

While the traction mode, P_t^* is positive: two cases are examined. If P_t^* is lower than *Th3*, function of the *SOC* (*Th3* becomes null if *SOC* is lower than a minimum value), then the electric mode is activated (the ICE is stopped and the clutch1 is opened). If P_t^* is greater than *Th4*, function of the SOC, then the ICE is started. In this case, when the storage system *SOC* is greater than the threshold *Th1*, then no serial flux is required and the boost mode is fully allowed beyond the ICE capabilities. However, if the *SOC* falls under the threshold *Th2*, than the serial flux is activated with an amount of power recharging the storage system function of the SOC. This amount is limited by a high value

corresponding to the SS power limit and a low value for efficiency reasons. In this case the boost mode is progressively inhibited if the *SOC* is decreasing below *Th2*.

While the regenerative mode, P_t^* is negative and the electric mode is always activated unless the *SOC* becomes greater than a maximum value SOC_{max}. In this last case, recharging battery is forbidden and the ICE brake mode is activated by closing the clutch1.

The same laws have been used for the three HEVs tested. For the batteries, the *SOC* variable (in %) corresponds to the following equation.

$$SOC(T) = SOC(t_0) - \frac{100 * \int_0^T I_{bat}(t)\eta_F dt}{Q_n} \qquad (7)$$

Where η_F is the Faradic efficiency (1 for positive current and 0.95 for negative current), Q_n is the nominal capacity (in As).

For the Ultra-capacitors the SOC is given directly by the voltage value. Thresholds Th_1 and Th_2 are fixed as the maximum and the minimum Voltage functioning limits.

G. HIL control

The HIL control of the parallel HEV configuration is performed using the simulink models of the simulated parts, a real time interface to adapt input and output signals, and actual components with their input demands (reference variables noted with '*') and their sensors (Fig. 7).

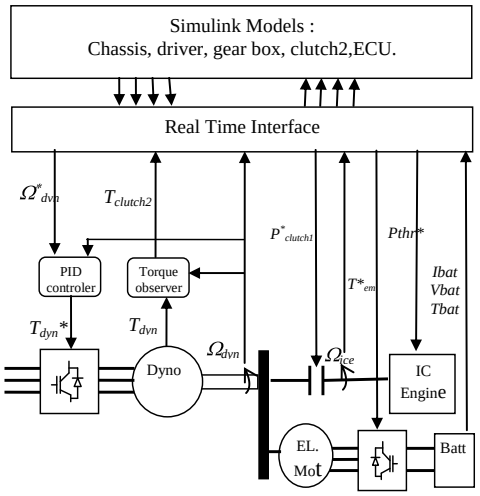

Fig. 7. Diagram of the HEV HIL control

At each sample time, the driver model gives the reference torque to be provided by the transmission, by comparing wheels target and actual speeds. Using the energy management implemented, this torque is split into an ICE torque demand T^*_{ice} and an EM torque demand T^*_{em}. The ICE torque demand is then converted into a throttle demand P^*_{thr} using a map and communicated to the Engine ECU through the real time interface. The EM torque demand is limited by the BMS (Battery Management System) using battery current, voltage and temperature measurements. Then the limited torque is transmitted to the EM inverter. Two modes are distinguished:

1) Electric mode: this mode is suggested by the simulated energy management and generates the following demands:

- T^*_{ice} =0 => P^*_{thr}=0 (throttle demand)
- Ignition* =0 => ICE stop.
- T^*_{em}=T^*_{driver}
- $P^*_{clutch1}$=1 (open).

2) Hybrid mode: In this mode the reference variables become:

- T^*_{ice} =k T^*_{driver} => $P^*_{thr} = f(T^*_{ice}, \Omega_{ice})$
- T^*_{em} =(1-*k*) T^*_{driver} (k>1 : serial flux, k<1 boost mode)
- Ignition*=1
- $P^*_{clutch1}$=0 (locked).

In the hybrid mode (most general case), the two actual torques of the ICE and the EM are coupled through a transmission belt and transmitted to the dynamometer shaft. Using a PID controller, the *dyno* imposes a resistant torque in order to follow the reference speed generated by the simulation model.

Generation of the reference dyno speed :

A torque sensor on the *dyno* allows an accurate measurement of the torque T_{dyn}. In order to estimate correctly the torque actually applied on the shaft, the measured torque is compensated using a torque observer and the *dyno* inertia identified value. The torque observed is exactly that needed to be applied to the clutch2 primary shaft in the simulation model, and corresponds to the summation of the actual ICE and EM torques. When applying this torque, and according to clutch2 state, the wheels torque is calculated using gear box model and the instantaneous gear ratio imposed by the ECU. The chassis model allows the vehicle speed calculation (equation 1) and consequently the rotating speed of the primary plate of clutch2 when it is locked. When it is slipping (hybrid mode and ICE rotating speed < secondary clutch2 plate speed), clutch2 primary speed is calculated locally using the clutch position and the transmissible torque of the equation 4. In the two cases, it is that speed which is used as a reference for the *dyno* speed.

The corresponding vehicle (wheels) speed is used to generate the next driver reference torque according to the equation 6.

To conclude this section, we can say that the key variables to connect the real time simulation model to the tested components are the estimated ***clutch2 torque*** (as input) and the clutch2 primary calculated ***speed*** as the reference for *dyno* speed.

IV. EXPERIMENTAL RESULTS

A. Dyno and ICE Control

In order to validate the whole HIL control, one should verify that the calculated speed imposed by the model causality through the vehicle inertia is well respected by the *dyno* performance. The Fig. 8 represents, for the extra urban part of the NEDC, the calculated primary speed of clutch2 (*dyno* speed reference) and the measured speed performed by the *dyno* on the actual shaft.

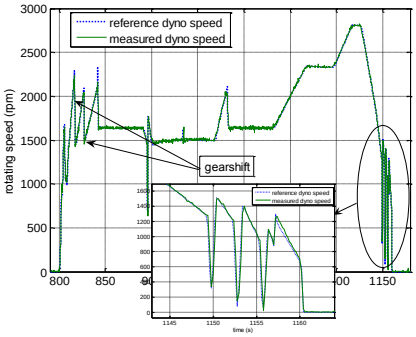

Fig. 8. Reference and measured speed of the dyno during the HIL simulation of the parallel HEV. Extra urban sequence of the NEDC.

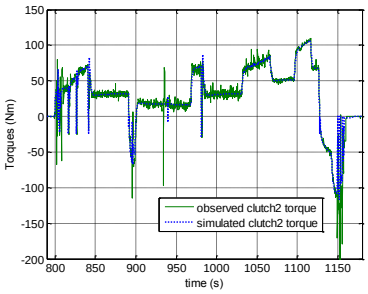

Fig. 9. Observed and simulated clutch2 torques.

As illustrated in Fig 8, the *dyno* speed is well controlled, even during the gearshift phases where the speed variations are relatively fast (see enlarged graph).

This issue being checked, one should also examine clutch2 primary torque behaviour and its coherence with the all simulation model results (Fig. 9). Even if some transient torques are under-estimated in simulation, mainly during the clutching phases (e.g. section III. D), we can note a good concordance between the real time observed torque and the simulated one.

At this step of the work, we can estimate that the instantaneous power performed by the *dyno* corresponds well to the simulated power required by the vehicle and provided by the actual components.

B. Regenerative braking Limitation for the HEV1

Figure 10 shows experimental results concerning electric motor torque for the HEV1 during a sequence of the NEDC driving cycle.

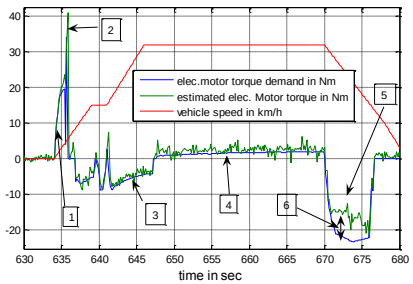

Fig. 10. experimental motor torque demand and response for HEV1.(same sequence)

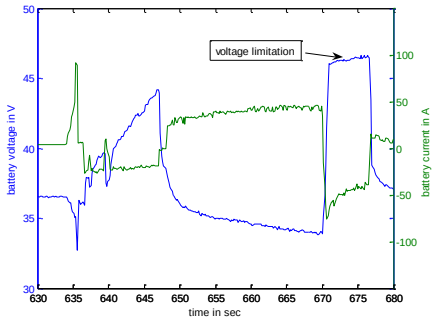

Fig. 11. Voltage and current of the lead acid battery for HEV1.(same sequence)

We can observe the following phases:

1- Electric mode when the vehicle starts to move,

2- ICE cranking with an extra torque demand. Here the power demand threshold of the hybrid mode is reached,

3- ***Serial flux*** for battery SOC balancing,

4 - Electric mode during low power demand (steady speed),

5- Regenerative braking mode.

In this last phase (5), one could note that the reference EM torque is not respected, as it is shown in zone 6 of Fig. 10. This behaviour is due to a voltage limitation of the lead acid battery during the recharging phase (Fig. 11).

Above this limit, battery voltage increase may entail water dissociation into hydrogen and Oxygen. It appears that this issue limits considerably the charge acceptance of the sealed type lead acid battery and consequently the expected fuel economy of the HEV1 is also limited. This is not the case for HEV2 and HEV3 as it is explained in the next section.

C. Power and energy performance comparison of the three SS

The figures 12 and 13 represent the powers delivered by the three storage systems during urban and extra –urban sequence of the NEDC cycle.

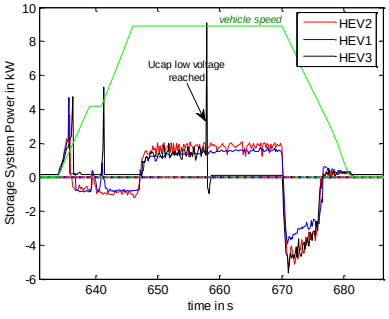

Fig. 12. Power of the 3 storage systems (urban sequence)

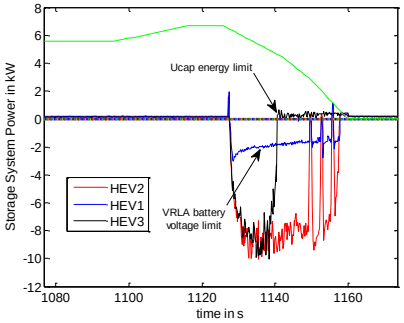

Fig. 13. Power of the 3 storage systems (extra-urban)

Globally, the same behaviour in term of energy management can be observed for the three HEVs which is in concordance with the algorithm described in the section III.F. Only the thresholds are different and lead to local differences such as ICE start for HEV3 at 658s because of low Ultra-capacitors voltage limit. We can also see the same phenomenon described in the previous section concerning HEV1 and emphasised in the last deceleration of the second sequence (fig. 13). For the HEV3, the regenerative power is not limited but as we can expect for the Ultra-capacitors, energy limitation is observed during the last deceleration of the cycle. Only HEV2 presents no limitation of its power and energy performance on this cycle.

For the energy variation of the three storage systems, we have plotted the SOC of the batteries and the Ultra-cpacitors voltage during a nearly balanced NEDC cycle (figure 14 and 15)

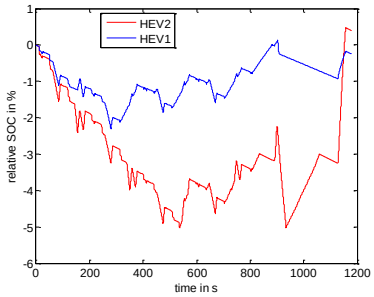

Fig. 14. Batteries relative SOC of HEV1 and HEV2.

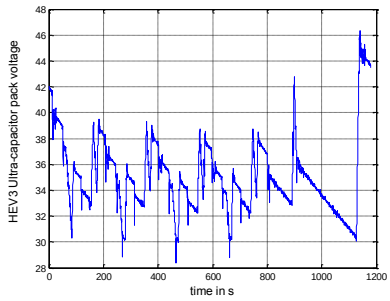

Fig. 15. Ultra-capacitors voltage of HEV3 on NEDC.

We can note that for HEV2, Energy recovery capabilities allow a deeper use of the batteries and then more electric mode at low speed, which is not the case for the HEV1. For the ultra-capacitors, only instantaneous power is important and the energy management is reduced to voltage limits management.

In the next section we will highlight the weight of these power and energy behaviour on the fuel economy results.

D. Fuel consumption and (CO2,NOx) emission of the three HEVs

The fuel consumption and the pollutants emission (CO, HC, NOx) are measured using an industrial device based on Constant exhaust gas Volume Sampling (CVS). Chemical equations of the fuel combustion allow fuel consumption calculation using the measured gases concentrations. In addition, a fuel balance is used to evaluate the fuel mass consumed during the entire cycle and this value is correlated with the CVS calculation.

In order to evaluate the fuel economy performance of the HIL simulated HEVs, one must compare HIL simulated conventional vehicle consumption with the HEVs one, obtained at battery balanced SOC (ie final SOC=initial SOC). As it is difficult to obtain experimentally a perfect zero ΔSOC (called SOC deviation on the figures), the different driving cycles are performed several times with different initial SOC. Then the consumption at zero SOC deviation is estimated using linear interpolation. Fig. 16 presents the relative consumption results of the HEV1, 2 and 3 for a HYZEM urban driving cycle [17]. For the Ultra-capacitors case (HEV3, fig 16 c), the fuel consumption is not sensitive to the SOC (here equivalent to the voltage), because of the low amount of energy available in this type of storage system.

For the three cases, the relative consumption values are the measured consumptions divided by the mean value of the reference vehicle consumptions.

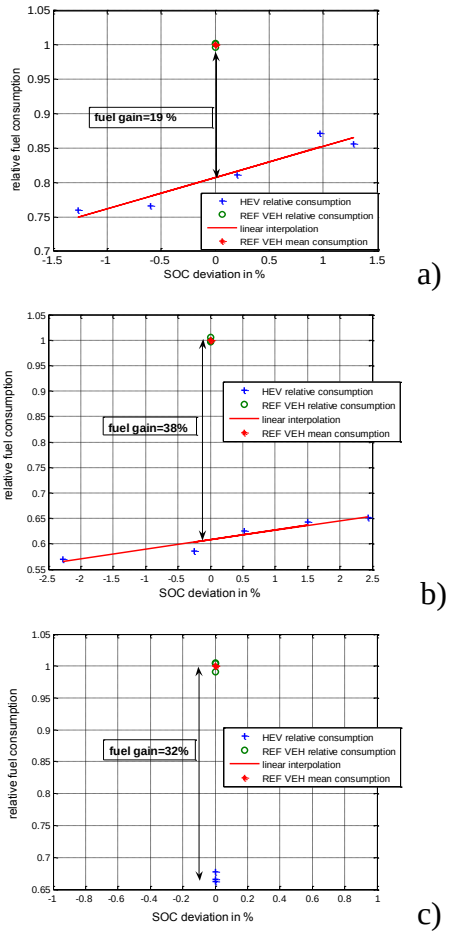

Fig. 16. Urban Relative fuel consumption versus the SOC deviation of the storage system. a) HEV1, b) HEV2, c) HEV3.

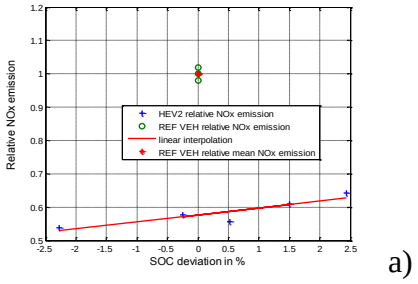

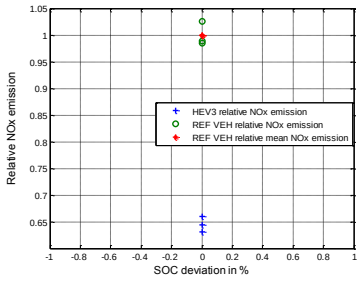

b)

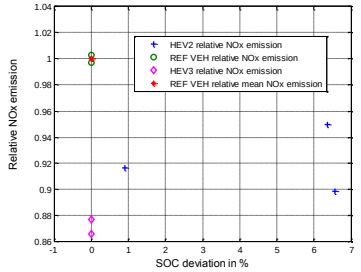

c)

Fig. 17. Measured NOx emission versus the SOC deviation of the storage system. a) HEV2,urban cycle, b) HEV3, urban cycle, c) HEV2 and 3, road cycle.

In urban conditions, notable fuel economy is registered for the 3 HEVs with a more important advantage for the HEV2 and HEV3. Concerning NOx, HEV2 and HEV3 (HEV1 data is not available) lead to lower emission than the reference vehicle in urban use, which is interesting for diesel engine. However, as shown in figure 17 c), NOx emission reduction is much more discussable in road condition and results should be analysed with caution because of the relatively high error on this type of measurement (2 different values at almost the same SOC variation for HEV2).
In term of CO2 emission, which is the most important and urgent problem to solve nowadays, the table 3 summarizes the performances of the three HEVs compared to the reference vehicle.

TABLE III
CO2 EMISSION OF THE REFERENCE VEHICLE AND THE 3 STUDIED HEVS ACCORDING TO THE DRIVING CYCLE.

	Ref VEH	HEV1		HEV2		HEV3	
	CO2 (g/km)	CO2 (g/km)	Gain (%)	CO2 (g/km)	Gain (%)	CO2 (g/km)	Gain (%)
NEDC Warm	105.7	89.0	15.2	83.4	21.1	83.6	18.8
URBAN	137.8	108.8	19.3	84.3	38.7	89.9	32.8
ROAD	114.3	104.9	8.0	97.2	14.9	101.8	8.7
HIGH-WAY	130.5	130.8	-0.2	129.5	0.7	130.2	0.2

We can note that the reference vehicle presents already low CO2 emission thanks to its diesel engine. Hybridization however allows appreciable gains mainly in urban use and especially for HEV2 and HEV3 with less than 90 g/km of CO2 emission. The most efficient solution for all kind of use is HEV2.

E. Comparison of PHIL with simulation for HEV1

In order to highlight PHIL approach advantages, one should compare experimental results to those obtained by pure simulation. Table IV summarizes fuel consumption gain predicted by the simulation model for HEV1, compared to experimental values obtained in the PHIL configuration.

TABLE IV
COMPARISON OF FUEL CONSUMPTION GAIN FOR HEV1: SIMULATION AND PHIL.

	Simulated fuel Consumption gain (%)	Measured fuel Consumption gain (%)	Error (%)
NEDC	12	15	20
Urban	24	19	26
Road	7	6	16
highway	-1	#0	/

One could note that even if the fuel consumption gain values are of the same order and have the same variations, the estimated error between simulation and PHIL could be relatively important. Some elements of explanations could be given by the curves represented in Fig. 18, corresponding to an urban sequence of the NEDC cycle.

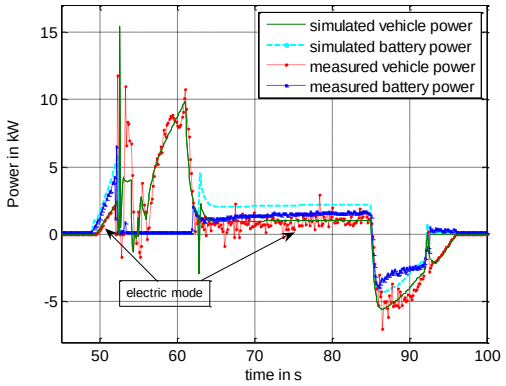

Fig. 18. Simulated and measured vehicle and battery powers. HEV1 Configuration.

In fact, we can see that, although the vehicle power is sensitively the same, the electric mode in simulation requires more power from the battery than recorded in the experiment. Consequently, the simulation model over-estimates the losses of the electric drive train and thus under-estimates the fuel economy. This is specially valid for the NEDC cycle where low steady speeds are frequent in the first part of the cycle.
For the HYZEM urban cycle, this advantage for the actual electric drive train is widely compensated by the battery charge acceptance problem discussed in the section IV.B. This phenomenon, not already taken into account in our simulation, entails more frequent voltage limitation in the urban cycle and then leads to a fuel consumption gain clearly lower than that predicted by simulation.

V. CONCLUSION

A PHIL approach has been applied to a parallel HEV configuration in order to simulate some parts of the vehicle and test in the same real time process the key components of the hybrid powertrain.

The implementation of this approach in a high dynamic test bench has been detailed and validated. It allowed us to check the effectiveness of the fuel consumption gain, predicted by simulation, using a rule based energy management law.
Three storage systems: a lead acid battery, a NiMH battery and an Ultra-capacitor, have been tested and compared in term of fuel consumption and pollutants emission using the same vehicle characteristics and the same experimental conditions. NiMH batteries showed more important latitude for recharge acceptance and energy cycling, leading to the largest fuel economy among the three configurations. Ultra-capacitors could be also an interesting trade off between cost and CO2 benefits for hybrid vehicle without ZEV mode. However, the low cost solution using lead acid batteries (100 to 200 Euros per kWh [18]) presents low recharge acceptance and their life cycling performance is also relatively low. This type of batteries, considered as the most mature and available technology is also pointed as the greatest potential of pollution [27, 30]. The NiMH Batteries are considered also as a mature and safe solution thanks to Toyota and Honda HEVs experience during the last decade. However ultracapacitors, although the possible cost advantage compared to NiMH batteries, present less maturity and safety should be also improved.
Finally, as perspectives, advanced energy management strategies studied by simulation will be implemented on the PHIL test bench [25, 26]. They particularly would give us more information on the NOx emission behaviour and if it is necessary or not to integrate them in the optimisation criterion for diesel HEVs.

Appendix:
AVL: Austrian test bench manufacturer.
BMS: Battery management system.
CIDI: Compressed Ignition Direct Injection.
ECU: Engine control unit.
EM: Electric motor.
ICE: Internal combustion engine.
HEV: Hybrid electric vehicle.
HYZEM: a set of driving cycles recorded in Europe.
NEDC: New European driving cycle.
PHIL: Power Hardware In the Loop.
SS: Storage system.
SOC: State of charge.
VEHLIB: Simulation library for vehicle dynamics and consumption.
VRLA: Valve regulated lead acid.
ZEV: Zero Emission Vehicle.

REFERENCES

[1] Ali Emady & Srdjan M. Lukic. *Topological Overview of Hybrid Electric and Fuel Cell Vehicular Power System Architectures and Configurations*. IEEE transaction on vehicular technology. Vol 54, N°3 May 2005.

[2] M. Eshani, Y. Gao, S. E. Gay, A. Emadi, "Modern electric, hybrid electric and fuel cell vehicles", *CRC Press*, New York, 2005.

[3] Srdjan M. Lukic & Ali Emady. Effects of Drivetrain Hybridization on Fuel Economy and Dynamic Performance of Parallel Hybrid Electric Vehicles. IEEE transaction on vehicular technology. Vol 54, N°3 May 2005.

[4] B. Jeanneret, R. Trigui, F. Badin, F. Harel, "New Hybrid concept simulation tools, evaluation on the Toyota Prius car", *EVS'16*, Beijing (China), October 1999.

[5] R. Trigui, B. Jeanneret, F. Badin, "Systemic modelling of hybrid vehicles in order to predict dynamic performance and energy consumption. Building the VEHLIB library of models", (text in French with abridged version in English), *RTS Journal*, November 2003.

[6] T. Markel, A. Brooker, T. Hendricks, V. Johnson, K. Kelly, B. Kramer, M. O'Keefe, S. Sprik, K. Wipke. NREL *Advisor. A systems Analisis Tool for Advanced Vehicle Modeling*. Journal of power sources (2002).

[7] Rousseau, A., and Pasquier, M. *"Validation Process of a System Analysis Model: PSAT,"* SAE paper 01P-183, SAE World Congress, Detroit (March 2001).

[8] Sung Chul Oh. "*Evaluation of motor characteristics for hybrid electric vehicles using the HIL concept"*. IEEE transaction on vehicular technology. Vol 54, N°3 May 2005.

[9] A. Bouscayrol, M. Pietrzak-David, P. Delarue, R. Peña-Eguiluz, P. E. Vidal, X. Kestelyn, "Weighted control of traction drives with parallel-connected AC machines", *IEEE Transactions on Industrial Electronics*, Vol. 53, no. 6, pp. 1799-1806

[10] Sung Chul Oh and Ali Emadi. Test and simulation of Axial Flux Motor Characteristics for Hybrid EVs. IEEE Transaction on Vehicular Technology, Vol. 53, No. 3, May, 2004. Pp. 912-919.

[11] H. Li, M. Steurer, S. Woodruff, K. L. Shi, D. Zhang, "Development of a unified design, test, and research platform for wind energy systems based on hardware-in-the-loop real time simulation", IEEE trans. on Industrial Electronics, vol. 53, no. 4, June 2006, pp. 1144-1151.

[12] A. Bouscayrol, X. Guillaud, P. Delarue, B. Lemaire-Semail, ?Energetic Macroscopic Representation and Inversion-Based Control Illustrated on a Wind Energy Conversion Systems Using Hardware-in-the-Loop Simulation, IEEE Transactions on Industrial Electronics, Accepted for future publication.

[13] Yonghua Cheng, Van Mierlo Joeri, and Philippe Lataire. Research and test platform for hybrid EV with supercapacitor based energy storage. 12th European Conference on Power Electronics and Applications. Aallborg, Denmark, September 2-5 2007, pp. 152.

[14] Wang Xiaoming, Chen Xi, Zhao Chunming, Wu Zhixin. Development and research on Harware-in-the loop Simulation System for HEV Powertrain. Automotive Engineering, Vol. 3, 2006, pp.221-224.

[15] Luo Yugong, Yang Diange, Jin Dafeng,Li Keqiang, Lian Xiaomin. Development of Powertrain Controller for Mild Hybrid Electric Vehicle, Chinese Journal of Mechanical Engineering, Vol 7, 2006, pp.98-102.

[16] Chu Liang, Wang Qingnian, Liu Minghui. Control Algorithm Development for Parallel Hybrid Transit Bus. Proceedings of IEEE Conference on Vehicle Power and Propulsion. Sept. 7-9, 2005, pp. 196-200.

[17] M André, European Development of hybrid technology approaching efficient zero emission mobility (HYZEM), INRETS Report N°: LEN 9709. 1997.

[18] Passier G., Conte F. V., Smets S., Badin F., Brouwer A., Alaküla M., Santini D., Alexander M. Status Overview of Hybrid and Electric Vehicle technology (2007). Final report phase II, Annex VII IA-HEV, International Energy Agency.

[19] http://www.avl.com/wo/webobsession.servlet.go/encoded/YXBwPWJjbXMmcGFnZT12aWV3Jm1hc2s9ZG93bmxvYWQmbm9kZXRpdGxlaWQ9MzY0ODYmbm9lbmNv_0AZGU9UERG.pdf

[20] B. Jeanneret, R. Trigui, B. Malaquin, M. Desbois-Renaudin, F. Badin, C. Plasse, Jscordia. "*Mise en œuvre d'une commande temps réel de transmission hybride sur banc d'essai moteur »*. 2nd European conference : Alternatives énergétiques dans l'automobile. Avril 2004, Poitiers France.

[21] Scordia J., Desbois Renaudin M., Trigui R. (2004) Hybrid power train sizing and potential consuption gains. **In** IEEE: *IEEE VPP 2004 - International Symposium on Vehicular Power and Propulsion*, Paris, France, October 6-8, 2004.

[22] Delprat S., Lauber J., Guerra T-M., Rimaux J. (2004). Control of a parallel hybrid powertrain: optimal control. *IEEE Transactions on Vehicular Technology*, 53 (3), pp. 872-881.

[23] W. Lhomme, R. Trigui, P. Delarue, B. Jeanneret, A. Bouscayrol, F. Badin. Switched causual modeling of transmission with clutch in hybrid electric vehicles. IEEE transaction on Vehicular Technology. Vol. 57, N. 4. pp 2081-2088.

[24] W. Lhomme, R. Trigui, A. Bouscayrol, P. Delarue, B. Jeanneret, F. Badin (2008) Inversion-Based Control of a Vehicle with a Clutch using a Switched Causal Modelling. International Journal of Systems Science. (accepted, to be published).

[25] Kermani S., Delprat S., Trigui R., Guerra T. M. (2007). A comparison of two global optimization algorithms for hybrid vehicle energy management. IFAC IEEE International conference on advances in vehicles and safety ACVS07. Buenos Aires, Argentina. February 8-10 2007.

[26] Kermani S., Delprat S., Trigui R., Guerra T. M. (2008). Predictive energy management of hybrid vehicle. IEEE Vehicular Power and Propulsion Conference. September 3-5 2008 Harbin, China.

[27] Ahmed Pesaran, Jeff Gonder, Matt Keyser. Ultaracapacitor Applications and Evaluation for Hybrid Electric Vehicles.. 7th Annual Advanced Capacitor World Summmit Conference 2009, La Jolla, California, US.

[28] Andrew F. Burke. Batteries and Ultracapacitors for Electric, Hybrid, and Fuel Cell Vehicles.Proceedings of the IEEE. Vol. 95, No. 4, April 2007.

[29] Andrew F. Burke. Ultracapacitors: why, how, and where is the technology. Journal of Power sources. No 91, 2000. pp. 37-50.

[30] C. C. Chan, Liqing Sun, Ruchun Liang, and Qingeai Wang. Current Status and Future Trends of Energy Storage System for Electric Vehicles. Journal of Asian Electric Vehicles. Volume 5, Number 2, December 2007.

Rochdi Trigui was born in Sfax, Tunisia, in 1969. He received the diploma of Electrical Engineer from the National High School of Electrical and Mechanical Engineering of Nancy France in 1993 and his Phd degree in electrical engineering in 1997 from the Polytechnic National Institute of Lorraine. Since 1998, he is researcher in the French National Institute for transport and safety Research (INRETS), in the field of electric and hybrid vehicles. He is currently member of the French network MEGEVH for hybrid vehicles and components modelling and IEEE VTS member.

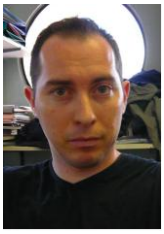

Bertrand Malaquin is an Engineer Assistant in charge of hybrid test bench at INRETS, since 2002. He has worked previously for one year as technical assistant in APAVE France. He received his Assistant Engineer degree in 2001 in the field of materials and controls.

Bruno Jeanneret has received his Engineering degree from INSA of Lyon in 1989. Since 1993 he is Engineer in the National Institute for transport and safety research (INRETS), France. He is currently working on hybrid and electric vehicles modelling and components testing.

Cedric Plasse is 43 years old and is graduated of the Université Technologique de Compiègne (UTC) (1992). He has worked since 1992 at Valeo. He successively held the positions of design engineer, project leader for the development of new generators and director of electronic R&D at Valeo Electrical Systems. He is now director of alternators and regulators projects at Valeo Engine & Electrical Systems.